

We are IntechOpen, the world's leading publisher of Open Access books Built by scientists, for scientists

6,900

Open access books available

185,000

International authors and editors

200M

Downloads

Our authors are among the

154

Countries delivered to

TOP 1%

most cited scientists

12.2%

Contributors from top 500 universities



WEB OF SCIENCE™

Selection of our books indexed in the Book Citation Index
in Web of Science™ Core Collection (BKCI)

Interested in publishing with us?
Contact book.department@intechopen.com

Numbers displayed above are based on latest data collected.
For more information visit www.intechopen.com



Swelling Elastomers: Comparison of Material Models

Sayyad Zahid Qamar, Maaz Akhtar and Tasneem Pervez

IntechOpen

*I think all literature should be read as comparative literature.
And I think we should write out of what we know, but in the expectation that
we can be changed at any moment by something we have yet to discover.
Margo Jefferson*

Abstract

Little data is available about the material properties and swelling response of the elastomers used in swell packers. This information is necessary for modeling and simulation of these elastomers in different petroleum applications. An experimental setup was therefore designed and implemented at Sultan Qaboos University (SQU) to investigate the material behavior of these elastomers under tension and compression, so that these properties could be used for different simulations. Before developing a finite element model (FEM) of elastomer seal performance, it was felt that a thorough evaluation needs to be carried out to decide which of the currently available material models is most suitable for swelling elastomers. This comparison translates into the selection of the correct strain energy function for accurate determination of material coefficients. Different hyperelastic material models are compared here. Experimental investigations under tensile and compressive loads, along with their numerical analysis are presented in detail in this chapter.

Keywords: Swelling elastomer, finite element simulation, material model, model comparison

1. Introduction

Metallic and rubber seals have been used for quite some time in oilfield development. However, the advent of swelling elastomer seals has revolutionized the technology. Deployment of swelling elastomers in a variety of petroleum applications are discussed in detail in Chapter 2. Before using swelling elastomers for any application, behavior under different fluids and environmental conditions should be known to predict the actual response. It can be done experimentally, analytically, or through numerical simulations. Though it would be most efficient time-wise, no analytical work is available that entirely explains the behavior of these materials. On the other hand, it is difficult, costly, and time-consuming (and at times even impossible) to perform experiments for all the possible conditions. Hence, a robust numerical simulation strategy, validated against experimental results, can be used to predict the behavior of swelling elastomers.

Little data is available (about their material properties and swelling response), which is needed for modeling and simulation of these elastomers in different

petroleum applications. An experimental setup was therefore designed and implemented at Sultan Qaboos University (SQU) to investigate the material behavior of these elastomers under tension and compression, so that these properties could be used for different simulations. Before developing a finite element model (FEM) of elastomer seal performance, it was felt that a thorough evaluation needs to be carried out to decide which of the currently available material models is most suitable for swelling elastomers. This comparison translates into the selection of the correct strain energy function for accurate determination of material coefficients. Different hyperelastic material models are compared here. Experimental investigations under tensile and compressive loads, along with their numerical analysis are presented in detail in this chapter.

2. Models for rubberlike materials

Rubber elasticity theory explains the mechanical properties of a rubber in terms of its molecular constitution. This approach involves two essentially separate issues. First is the treatment of the statistical properties of a single long-chain molecule in terms of its geometrical structure. Second comes the application of this treatment to the problem of the network of long-chain molecules corresponding to a cross-linked or vulcanized rubber.

First statistical mechanics approach to describe the force on a deforming elastomer network was based on Gaussian statistics. The basic assumption in this theory is that a chain never approaches its fully extended length. The problem was initially attempted by Kuhn and Grun [1] who derived a relation between elastic modulus and molecular weight. More precise treatment leading to explicit forms of stress–strain curves valid for large strains were developed by Wall [2], Flory and Rehner [3, 4], and, James and Guth [5]. Results show that these models fail to capture large and even moderate stretches. Hence many constitutive models were developed in an attempt to predict the behavior not only for small stretch levels but also for medium and large stretches.

Other researchers followed non-Gaussian statistics. These are physical models based on an explanation of a molecular chain network, phenomenological invariant-based and stretch-based continuum mechanics approach. The distinctive feature of non-Gaussian approach is that it presumes that a chain can attain its fully extended length. Phenomenological approach is used to relate empirical findings of certain phenomena in such a way that it is consistent with fundamental theory, but is not directly derived from theory. This approach is further divided into stretch-based and invariant-based models. Invariants are basically defined by principal stretches. Models in which stretches can be written in terms of invariants are classified as invariant-based models, while models that cannot be converted into invariants are known as stretch-based models. Micromechanical models describe a material as a three-dimensional network and consider statistical mechanics arguments on networks of cross-linked long-chain molecules. A hyperelastic material model is a type of constitutive relation for rubberlike materials in which the stress–strain relationship is developed from a function. Most continuum mechanics treatment of rubber elasticity begins with assuming rubbers to be hyperelastic and isotropic in nature. **Figure 1** gives a broad classification of different types of hyperelastic material models.

2.1 Micromechanical models

These models assume a unit cell which deforms in a principal-stretch space to relate individual chain stretch to applied deformation. Wang and Guth [6] proposed

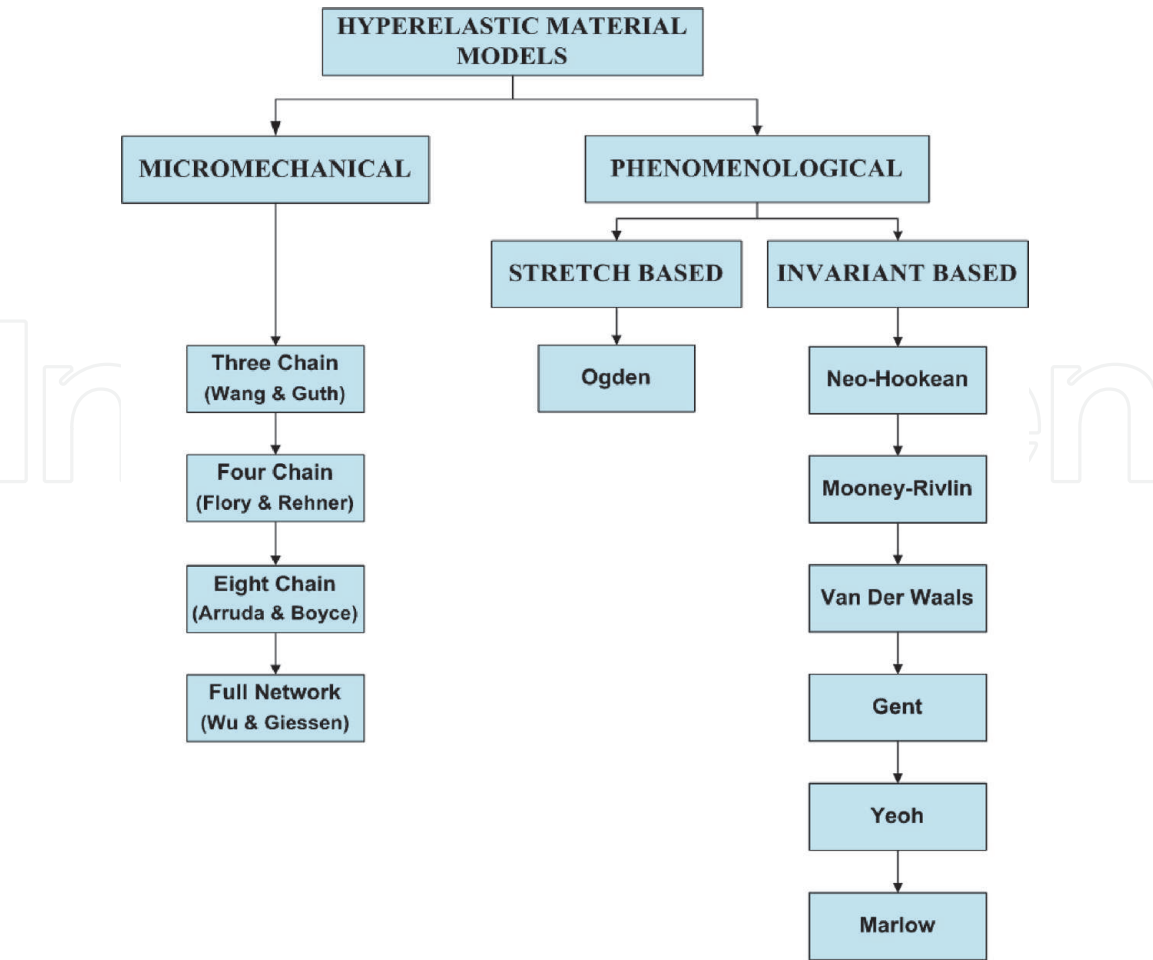


Figure 1.
General classification of different hyperelastic material models.

a three-chain model in which chains are located along the axes of cube. The chains deform affinely with the cell, and stretch of each chain corresponds to the principal stretch value. The strain energy function is given by

$$W_{3-Chain} = \frac{NkT}{3} \sqrt{n} \left[\lambda_1 \beta_1 + \sqrt{n} \ln \left(\frac{\beta_1}{\sinh \beta_1} \right) + \lambda_2 \beta_2 + \sqrt{n} \ln \left(\frac{\beta_2}{\sinh \beta_2} \right) + \lambda_3 \beta_3 + \sqrt{n} \ln \left(\frac{\beta_3}{\sinh \beta_3} \right) \right]$$
$$\beta_i = \mathcal{L}^{-1} \left(\frac{\lambda_i}{\sqrt{n}} \right); i = 1, 2, 3. \tag{1}$$

Here, \mathcal{L}^{-1} is the inverse Langevin, N is the chain density, k is the Boltzman constant, T is the absolute temperature, n is the length of chain, and λ_i are the principal stretches. Three-chain model closely follows experimental data only for uniaxial case, and only for small deformations under shear. Flory and Rehner [3, 4] developed a four-chain tetrahedral model. Later, Treloar [7] attempted to determine the entropy of deformation using numerical method of computation, in which four chains are linked together at the center of a regular tetrahedron. Tetrahedron deforms according to the applied deformation and chains deform in un-affine manner. Four chain (tetrahedral) model gives good match with experimental data for uniaxial and shear cases, but extrapolates beyond the actual stretch region. For biaxial data, three-chain and four-chain models do not yield convincing results. Relationship between the stretches of individual chain to the applied stretch for the four-chain model is determined by an iterative method, hence expression for strain energy function is not provided here.

Arruda and Boyce [8] proposed an eight-chain model in which chains align along diagonals of a unit cell. Due to the symmetry of chain structure, the interior junction point remains at the center throughout the deformation. Strain energy function is given by

$$W_{8-Chain} = \frac{NkT}{3} \sqrt{n} \left[\lambda_{Chain} \beta_{Chain} + \sqrt{n} \ln \left(\frac{\beta_{Chain}}{\sinh \beta_{Chain}} \right) \right]$$

$$\beta_{chain} = \mathcal{L}^{-1} \left(\frac{\lambda_{chain}}{\sqrt{n}} \right)$$

$$\lambda_{chain} = \left[\frac{1}{3} (\lambda_1^2 + \lambda_2^2 + \lambda_3^2) \right]^{1/2} \quad (2)$$

where, and, λ_{chain} is the chain stretch. Eight-chain model makes good predictions for large strain behavior under different states of deformation, but diverges beyond the actual stretch region for biaxial and shear cases.

Wu and Giessen [9] suggested a full network chain model in which chains are randomly distributed and deform in an affine manner. Strain energy response is determined by overall integration which is computationally intensive; expression for strain energy is therefore reproduced here. To develop constitutive relations, work done by the stresses is established in terms of strain energy function. Strain energy function must depend on the amount of stretch via invariants of the stretch tensor. The coefficients in these functions should be determined by uniaxial, biaxial, and shear test data. The essential problem is to determine the strain energy function for providing good fit with a number of sets of experimental data.

2.2 Phenomenological invariant-based models

One of the first attempts at a hyperelastic material model based on the phenomenological invariant-based approach was made independently by the two scientists Mooney [10] and Rivlin [11]. Due to the assumption of incompressibility, the third invariant is not considered, yielding the following expression for strain energy function:

$$W_{Rivlin} = \sum_{i+j=1}^{\infty} C_{ij} (I_1 - 3)^i (I_2 - 3)^j \quad (3)$$

By keeping only the second term of this expression, we get the famous Mooney-Rivlin model for elastomer deformation

$$W_{Mooney-Rivlin} = C_1 (I_1 - 3) + C_2 (I_2 - 3) \quad (4)$$

Mooney-Rivlin model makes passable predictions for uniaxial and shear cases in the low-stretch region, but does not yield good predictions for equibiaxial case and uniaxial and shear cases in the large-stretch region. As reported by Treloar [12] and Boyce and Arruda [13], when only the first term of Mooney-Rivlin strain energy function is retained, it becomes the neo-Hookean model:

$$W_{neo-Hookean} = C_{10} (I_1 - 3) \quad (5)$$

Kilian [14] explains that van der Waal hyperelastic material model gives the mathematical relation in terms of the initial shear stress ' μ_s ', global interaction

parameter 'a', effective invariant $\tilde{I} = (1 - \beta_v)I_1 + \beta_v I_2$ and the parameter $\eta_v = \sqrt{\frac{\tilde{I}-3}{\lambda_m^2-3}}$; β_v is known as the invariant mixture parameter:

$$W = \mu_s \left\{ -(\lambda_m^2 - 3) [\ln(1 - \eta_v) + \eta_v] - \frac{2}{3} a \left(\frac{\tilde{I} - 3}{2} \right)^{\frac{3}{2}} \right\} \quad (6)$$

Gent [15] proposed a new constitutive relation for strain energy function which is given by the expression

$$W = -\frac{E}{6} J_m \ln \left[1 - \left(\frac{J_1}{J_m} \right) \right] \quad (7)$$

where $J_1 = (I_1 - 3)$, and J_m is the maximum value for J_1 .

The Yeoh model [16] is derived from Rivlin strain energy function by expanding only the first three terms, and neglecting the second invariant, yielding:

$$W_{Yeoh} = C_{10}(I_1 - 3) + C_{20}(I_1 - 3)^2 + C_{30}(I_1 - 3)^3 \quad (8)$$

The Marlow hyperelastic material model [17] is another variation of this approach:

$$W = C(\lambda_1^2 + \lambda_2^2 + \lambda_3^2) = C(I_1) \quad (9)$$

Here, C is a material parameter, and λ is the principal stretch.

2.3 Phenomenological stretch-based models

Ogden model [18] proposes a strain energy function based on the principal stretches for incompressible materials. Principal stretches are directly measurable quantities and it is one obvious advantage of using them. Ogden strain energy function is given by

$$W = \sum_{n=1}^Q \frac{\mu_n}{\alpha_n} (\lambda_1^{\alpha_n} + \lambda_2^{\alpha_n} + \lambda_3^{\alpha_n} - 3) \quad (10)$$

where μ_n and α_n are material constants. Nonlinear least square optimization technique is used by Twizell and Ogden [19] to determine the stable constants for the above strain energy function and to find an improve fit to the data when 'n' increases. This model can be more accurate if data from multiple experiments are available.

There are various other forms of strain energy potentials (**Figure 1**) for modeling hyperelastic isotropic elastomers, such as the ones reported by Ali et al. [20], Hossain and Steinmann [21], and Steinmann et al. [22]. However, these functions seldom describe the complete behavior of these swellable materials, especially for different loading conditions.

2.4 Other models

Some researchers have attempted to develop material models which explain the stress-stretch behavior of an elastomer after swelling to a particular level. As

described by Treloar [23], Gauss model follows a molecular approach and involves swelling ratio ' v_s ':

$$W = \frac{NkT}{2} v_s^{\frac{1}{3}} (\lambda_1^2 + \lambda_2^2 + \lambda_3^2 - 3) \quad (11)$$

Increasing discrepancies between Gaussian theory and experiments have been recognized when moving from small to large stretch levels. This discrepancy is amplified when the effect of swelling is included. Flory and Erman [24] model predicts the swelling behavior reasonably well only for small to moderate stretches. Arruda-Boyce model (for stress-stretch behavior coupled with elastomer swelling) is based on a simplified representation of eight chains lying along the diagonal of a cubic cell. The Cauchy stress for Arruda-Boyce model [25] is given by the following relation:

$$\sigma = v_s^{\frac{2}{3}} \frac{NkT}{3} \frac{\sqrt{n}}{\lambda_c} \mathcal{L}^{-1} \left[\left(\frac{v_s^{-\frac{1}{3}} \lambda_c}{\sqrt{n}} \right) \left(\lambda^2 - \frac{1}{\lambda} \right) \right] \quad (12)$$

This model, when used for predicting swelling behavior of elastomers, gives close results only for large stretch. They later attempted to combine their model with Flory-Erman model. This hybrid model is supposed to take into account the actual effect of swelling for small to large stretches. However, even this hybrid model fails to replicate the actual behavior of swelling elastomers.

A few models have been proposed by authors such as Wagner [26]. These are basically hyperelastic models that also include swelling ratio, but fail to give reasonable predictions. There is hence a need for a model that predicts the actual behavior, and includes factors such as energy of mixing, and effect of diffusion, together with hyperelastic effect.

2.5 Energy-diffusion models

Other authors have suggested more realistic constitutive models for elastomers subjected to swelling, in which changes due to configuration entropy are considered along with energy of mixing and diffusion. According to Flory-Rehner theory [3, 4], free energy density can be written as the sum of strain energy density function due to thermodynamics of mixing and configuration entropy of polymer network. A number of authors use this concept to develop a relation for the prediction of swelling, such as Han et al. [27], Cai and Suo [28], Chester and Anand [29], Drozdov and Christiansen [30], Hong et al. [31], and Lucantonio et al. [32].

Flory-Huggins theory, proposed by Flory [33] and Huggins [34], considers the changes in entropy due to mixing. Changes due to configuration entropy are added by considering different available hyperelastic material models as discussed above. As explained by Lucantonio [32], Hong et al. [35], and Kang and Huang [36], solvent influx in swelling elastomer follows the diffusion phenomenon. A few authors, such as Biot [37], Cai et al. [38], Lucantonio and Nardinocchi [39], and Tomari and Doi [40], use the concept of porous media and assume swelling elastomer or gel to be poro-elastic. A porous material is made up of pores and its permeability is related to the pore size. Major portion of a swollen elastomer contains solvent which resists when under the influence of force. That is why models based on poro-elastic concept do not predict good swelling results in general as discussed by Hong et al. [31].

Most of the chemo-mechanical models use Gaussian-chain model for mechanical configuration changes that consider small stretching of chains, and use Fick's law to define fluid influx. Again, they give reasonable results only at small swelling levels. Material models for predicting swelling in polymer networks are discussed below.

2.5.1 Poroelastic models

Biot [37] used Darcy's law along with thermodynamics of mixing to model fluid influx into a porous medium (soil), the approach being known as poro-elasticity theory. This theory is used in a variety of applications to study porous materials from soils to tissues. Tomari and Doi [40] used the concept of poro-elasticity to develop a model for swelling dynamics. They assumed swelling time to be proportional to gel size, frictional constant, and changes in stresses. Barrière and Leibler [41] proposed a swelling model that is based on a porous media concept and includes frictional effect between elastomer and fluid. To describe fluid influx they use the dependence of coefficient of diffusion on concentration, and do not use Fick's law (as according to them it does not predict good behavior at large swelling). Cai et al. [38] performed experiments on swollen gel that is compressed between two plates. They developed a model using linear poro-elasticity for the experiments performed. Variational approach is employed by Baek and Pence [42] to investigate gels in equilibrium, subjected to loading on surface. They do not take into account the relationship for dynamical processes (like diffusion) prior to equilibrium. Lucantonio and Nardinocchi [39] describe bending due to swelling in a gel considering poro-elastic linear theory. Lucantonio et al. [32] investigated the stability between linear poro-elastic and nonlinear theory approaches assuming Gaussian statistics and homogenous configuration. Instead of considering dry state as reference configuration (like other models), they assume initially swollen elastomer as a reference state. Constitutive relations are derived using weak-form variational formulation. Bouklas and Huang [43] present a comparison of linear poro-elasticity and nonlinear Gaussian based (chemo-mechanical) theories. Both theories give similar results at small swelling ratios, but for higher swelling ratios linear theory fails and gives large errors as compared to nonlinear theory.

2.5.2 Chemo-mechanical models

Durning and Morman [44] use phantom network model along with Bastide's scaling model for taking into account the entropy changes due to configuration. Fick's law is used for describing fluid influx. Inconsistencies are present due to the use of Fick's law, as it does not provide a solution for nonlocal effects. Chemo-mechanical theory for hydrogels was developed by Dolbow et al. [45] and extended finite element method was implemented to study swelling. Continuum based sharp interface model and swelling kinetics for temperature sensitive stimulus responsive hydrogels was developed by Ji et al. [46]. Hong et al. [31] assume short and long range migration of solvent inside the polymer. Developed theory is based on non-equilibrium thermodynamics and considers free energy and kinetics to be material specific. They use Flory-Huggins theory to describe changes in free energy, while Gaussian approach is used for defining changes in entropy due to network configuration. They use the diffusion equation for fluid inflow of Feynman et al. [47], in which flux is proportional to gradient of chemical potential. Hong et al. [35] developed an equilibrium theory using Gibb's approach. Legendre transformation is used to represent the field in gel, analogous to compressible hyperelastic solid. Developed model is used on kinetics of fluid influx and Gaussian approach. User-defined subroutine (UHYPER) in ABAQUS is also developed for the model. Duda et al. [48]

follow Gibb's idea of multi-component solid for the development of an expression for swelling equilibrium. Theory is based on mechanics (macro) and chemistry (micro) of mixing of solid and fluid. They consider Gaussian neo-Hookean model for changes in configuration entropy of the elastomer. Development of the model assumes that the body is not fully immersed into the fluid. Kang and Huang [36] formulated a model based on variational approach to set governing equations combining chemical and mechanical conditions. They used similar approach as Hong et al. [31], following Gaussian-chain model for configuration entropy and Flory-Huggins equation for energy of mixing. They also develop an explicit formulation for tangent modulus and true stress. User-defined subroutine (UMAT) in ABAQUS is also developed for numerical investigation and comparison is done with user subroutine developed by Hong et al. [35].

A continuum mechanical theory along with fluid imbibition was developed by Chester and Anand [29]. They first use Gaussian approach to develop a model for swelling phenomenon. Fluid influx is taken into account using Darcy's law. Then they use micro mechanical non-Gaussian based approach for model improvement. As a further extension to their work, they include thermal effect and develop coupled equation for stretching, fluid influx, and heat transfer. Cai and Suo [28] use Flory-Rehner model to describe the changes in entropy due to stretching, but ignore the changes in entropy due to mixing of fluid and polymer. They develop an equation of state based on Gaussian-chain model considering stretching only. Yan and Jin [49] take into account the entanglements of chains, by using hybrid free energy function based on Edwards-Vilgis slip-link model and Flory-Huggins theory. Drozdov and Christiansen [30] propose a swelling model based on viscoelasticity and viscoplasticity. They study hydrogels, under both tensile and compressive loads, to investigate the effect of strain rate on elastic properties. Constitutive relations are based on viscoelasticity of gels.

All of the above models generally give reasonable results only for small swelling. For large swelling (as in the case of swelling elastomers), most of these models do not give close approximation to actual data.

3. Material models for swelling elastomers

None of the existing material models accurately represent the behavior of swelling elastomers. Different types of models for rubberlike materials were briefly described above. Major material models that can be used to represent stretchable elastomers, though not very accurately, are discussed in more detail in this section. As mentioned above, a swelling elastomer can be treated as a hyperelastic material, commonly modeled as an incompressible, homogeneous, isotropic, and nonlinear elastic solid. Due to its long and flexible structure, an elastomer has the ability to stretch to several times its initial length. Elastomers at small strains (up to 10%) have linear stress strain relation, and behave like other elastic materials [15]. In case of applications where large deformations exist, theory of large elastic deformation should be considered. Several theories for large elastic deformation have been developed for hyperelastic materials based on strain energy density functions. These models are based on phenomenological based continuum mechanics approach and micromechanically motivated network approach [20, 21]. Phenomenological models contain invariant-based or principal stretch-based approach usually containing polynomial functions. Micromechanical models typically have terms for cross-linked long-chain molecules [3, 4, 6, 8, 50]. Selection of appropriate strain energy potentials and correct determination of material coefficients are the main factors for modeling and simulation.

3.1 Gaussian Hyperelastic material models

One major approach used to define the deformations in elastomer chains follows Gaussian statistics, Neo-Hookean model being a good example. In Gaussian statistics, a chain never approaches the maximum stretch; rather, it is limited to small-to-moderate stretches. For a three dimensional polymer, due to its large chain density, probability distribution for any event x approaches a Gaussian distribution, given by

$$p(x) = \frac{1}{\sqrt{2\pi}\sigma_x} \exp\left(-\frac{x^2}{2\sigma_x^2}\right). \quad (13)$$

Standard deviation in terms of chain density (N) and distance between the chain ends (r) is given by Treloar [23] as

$$\sigma^2 = \frac{Nr^2}{3}. \quad (14)$$

Probabilities in x , y and z -directions are given by $p(x)$, $p(y)$ and $p(z)$, respectively. Knowing that

$$p(v) = p(x)p(y)p(z),$$

and assigning $b^2 = \left(\frac{3}{2Nr^2}\right)$, we get the following relation

$$p(v) = \frac{b^3}{\pi^{3/2}} \exp\{-b^2(x^2 + y^2 + z^2)\} = \frac{b^3}{\pi^{3/2}} \exp(-b^2r^2). \quad (15)$$

Here, (x_0, y_0, z_0) is the initial (unstretched) location, while (x, y, z) are the final coordinates in the stretched condition, and (obviously), $x^2 + y^2 + z^2 = r^2$. According to Boltzmann general principle of thermodynamics, entropy is proportional to the logarithm of the possible configurations corresponding to a specified state. For small volume ($dx dy dz$), probability can be used to define entropy (s) as follows:

$$\begin{aligned} s &= k \ln \frac{b^3}{\pi^{3/2}} \exp(-b^2r^2) dx dy dz \\ \Rightarrow s &= k \left[\ln \frac{b^3}{\pi^{3/2}} - b^2r^2 + \ln(dx dy dz) \right] \\ \Rightarrow s &= \text{constant} - kb^2r^2 \end{aligned} \quad (16)$$

where k is the Boltzmann constant. Taking change in unstretched end-to-end distance of chain ($x_o^2 + y_o^2 + z_o^2 = r_o^2$), and on simplification we get the change in entropy

$$\Delta s = kb^2\{x_o^2(\lambda_1^2 - 1) + y_o^2(\lambda_2^2 - 1) + z_o^2(\lambda_3^2 - 1)\}. \quad (17)$$

Taking summation for all chains, substituting $\sum x_o^2 = \sum y_o^2 = \sum z_o^2 = \sum r_o^2/3$ into Eq. (17), and on simplification we get

$$\Delta s = kb^2\{x_o^2\lambda_1^2 - x_o^2 + y_o^2\lambda_2^2 - y_o^2 + z_o^2\lambda_3^2 - z_o^2\}$$

$$\begin{aligned}\Rightarrow \Delta s &= -kb^2 \frac{r_o^2}{3} \{\lambda_1^2 + \lambda_2^2 + \lambda_3^2 - 3\} \\ \Rightarrow \sum \Delta s &= -\frac{kN}{2} (\lambda_1^2 + \lambda_2^2 + \lambda_3^2 - 3)\end{aligned}\quad (18)$$

Shear modulus for rubbers and elastomers is given by $G=NkT$. Helmholtz free energy is given by $W = -T\Delta s$, hence Eq. (18) can be written as

$$W = \frac{G}{2} (I_1 - 3), \quad (19)$$

where I_1 is the first invariant of stretch. Eq. (19) gives the strain energy function for neo-Hookean model [13, 23]. As it is derived using Gaussian statistics, it gives linear response for material where elastomer chain undergoes only small to moderate stretches.

3.2 Non-Gaussian Hyperelastic material models

Hyperelastic material models that follow non-Gaussian statistics consider that chains can stretch to reach maximum extensibility. Many models are formulated based on this approach, such as Mooney-Rivlin [10], Yeoh [16], Arruda-Boyce [8], Ogden [18], Gent [15], etc. Mooney-Rivlin model follows Valanis and Landel theory [51] according to which strain energy function for an isotropic material in finite deformation is of the form

$$W = f(\lambda_1) + f(\lambda_2) + f(\lambda_3). \quad (20)$$

Invariants based on principal stretches are given by

$$\begin{aligned}I_1 &= \lambda_1^2 + \lambda_2^2 + \lambda_3^2, \\ I_2 &= \lambda_1^2 \lambda_2^2 + \lambda_2^2 \lambda_3^2 + \lambda_1^2 \lambda_3^2,\end{aligned}$$

and

$$I_3 = \lambda_1^2 \lambda_2^2 \lambda_3^2. \quad (21)$$

For an incompressible isotropic material, third invariant vanishes and strain energy becomes a function of I_1 and I_2 only:

$$\begin{aligned}W(\lambda_1, \lambda_2, \lambda_3) &= C_1(\lambda_1^2 + \lambda_2^2 + \lambda_3^2 - 3) + C_2\left(\frac{1}{\lambda_1^2} + \frac{1}{\lambda_2^2} + \frac{1}{\lambda_3^2} - 3\right) \\ W &= C_1(I_1 - 3) + C_2(I_2 - 3).\end{aligned}\quad (22)$$

Eq. (22) gives the strain energy function for Mooney-Rivlin model, where C_1 and C_2 are material constants. According to this theory, stress-strain behavior depends upon the partial derivatives $\left(\frac{\partial W}{\partial I_1}, \frac{\partial W}{\partial I_2}\right)$. Characterization of elastic properties of a polymer consists of determining these partial differentials through experimental measurements. These partial differentials cannot be determined from experiments with only one deformation mode. Preferred methods are generally biaxial extension where stretches in both directions vary independently. Yeoh assumed that $\partial W / \partial I_1$ is much larger than $\partial W / \partial I_2$, so the second partial

derivative can be neglected. Strain energy function for Rivlin [11] can then be written as

$$W = \sum_{i+j=1}^{\infty} C_{ij} (I_1 - 3)^i (I_2 - 3)^j$$

$$\Rightarrow , W = \sum_{i=1}^{\infty} C_{ij} (I_1 - 3)^i \quad (23)$$

where index 'j' will always be zero. If the series is truncated after three terms, we get the expression for strain energy function for Yeoh model [16]:

$$W = C_{10} (I_1 - 3) + C_{20} (I_1 - 3)^2 + C_{30} (I_1 - 3)^3 \quad (24)$$

where C_{10} , C_{20} and C_{30} are material coefficients determined by fitting experimental data. If Eq. (23) is expanded only for 'i = 1', we get the Neo-Hookean strain energy function, in which $C_{10} = G/2$.

Another stretch based non-Gaussian phenomenological strain energy function for hyperelastic materials was proposed by Ogden [18]. This model is given by the following relation in terms of principal stretches:

$$W = \sum_{n=1}^Q \frac{\mu_n}{\alpha_n} (\lambda_1^{\alpha_n} + \lambda_2^{\alpha_n} + \lambda_3^{\alpha_n} - 3). \quad (25)$$

Here, ' μ_n ' and ' α_n ' are material constants that are determined by fitting the experimental data, and 'Q' is a positive definite integer. Material constants are related to shear modulus (G) by the following relation:

$$\sum_{n=1}^Q \mu_n \alpha_n = 2G. \quad (26)$$

Second degree Ogden strain energy function is given by expanding Eq. (24) for 'Q = 2':

$$W = \frac{\mu_1}{\alpha_1} (\lambda_1^{\alpha_1} + \lambda_2^{\alpha_1} + \lambda_3^{\alpha_1} - 3) + \frac{\mu_2}{\alpha_2} (\lambda_1^{\alpha_2} + \lambda_2^{\alpha_2} + \lambda_3^{\alpha_2} - 3),$$

$$\mu_1 \alpha_1 + \mu_2 \alpha_2 = 2G. \quad (27)$$

It is interesting to note that if Ogden model Eq. (24) is expanded for 'Q = 2' and for $\alpha_1 = 2$, $\alpha_2 = -2$, it gives an expression similar to the Mooney-Rivlin model:

$$W = \frac{\mu_1}{2} (\lambda_1^2 + \lambda_2^2 + \lambda_3^2 - 3) - \frac{\mu_2}{2} (\lambda_1^{-2} + \lambda_2^{-2} + \lambda_3^{-2} - 3)$$

$$\Rightarrow .W = \frac{\mu_1}{2} (I_1 - 3) - \frac{\mu_2}{2} (I_2 - 3) \quad (28)$$

Also, if Ogden model is expanded for 'Q = 1' with $\alpha_1 = 2$, $\alpha_2 = 0$, it reduces to the neo-Hookean model:

$$W = \frac{\mu_1}{2} (\lambda_1^2 + \lambda_2^2 + \lambda_3^2 - 3) = \frac{\mu_1}{2} (I_1 - 3). \quad (29)$$

Arruda-Boyce model [8] uses the statistical mechanics approach followed by many researchers [3, 4, 6, 50]. Instead of the 3-chain [6] and 4-chain models [3, 4]

of earlier researchers, Arruda-Boyce proposed a more accurate 8-chain approach, yielding the following strain energy function:

$$W = NkT\sqrt{n} \left[\beta_{chain} \lambda_{chain} + \sqrt{n} \ln \left(\frac{\beta_{chain}}{\sinh \beta_{chain}} \right) \right]. \quad (30)$$

Here, $\beta_{chain} = \mathcal{L}^{-1} \left(\frac{\lambda_{chain}}{\sqrt{n}} \right)$ is the inverse Langevin, N is the chain density, k is the Boltzman constant, T is the temperature, n is the chain length, and λ_{chain} is the chain stretch. Also, $G = NkT$ is the effective shear modulus.

Since $\mathcal{L}(x) = \coth(x) - \frac{1}{x}$, and $\coth(x) = \frac{1}{x} + \frac{1}{3}x - \frac{1}{45}x^3 + \frac{2}{945}x^5 \dots$, we can get

$$\mathcal{L}(x) = \frac{1}{3}x - \frac{1}{45}x^3 + \frac{2}{945}x^5 \dots$$

Also,

$$\mathcal{L}^{-1}(x) = 3x - \frac{9}{5}x^3 + \frac{297}{175}x^5 \dots$$

and

$$\sinh(x) = x + \frac{1}{6}x^3 + \frac{1}{20}x^5 - \frac{1}{5040}x^7 \dots \quad (31)$$

By showing that the expression for chain stretch reduces to a function of the first stretch invariant, $\lambda_{chain} = \sqrt{I_1/3}$, and using Eqs. 4.30 and 4.31, the final expression for Arruda-Boyce strain energy function becomes

$$W = G \left[\frac{1}{2}(I_1 - 3) + \frac{1}{20N}(I_1^2 - 9) + \frac{11}{1050N^2}(I_1^3 - 27) + \frac{19}{7000N^3}(I_1^4 - 81) + \dots \right]. \quad (32)$$

Gent [15] proposed an empirical constitutive relation using only two constants for the entire range of strains for hyperelastic materials. In statistical mechanics approach, when a chain reaches the fully stretched state, it is known as locking stretch. Gent describes this stretch as a maximum value of J_1 denoted by J_m , so that the strain energy function is given by the following relation:

$$W = -\frac{E}{6}J_m \ln \left[1 - \left(\frac{J_1}{J_m} \right) \right]. \quad (33)$$

Boyce [52] performed a comparison between Gent and Arruda-Boyce eight chain models. As $J_1 = (I_1 - 3)$ and $I_1 = \lambda_1^2 + \lambda_2^2 + \lambda_3^2$, Gent model can be expanded using natural logarithm.

$$\begin{aligned} W &= \frac{E}{6}J_m \left[\frac{J_1}{J_m} + \frac{1}{2} \left(\frac{J_1}{J_m} \right)^2 + \frac{1}{3} \left(\frac{J_1}{J_m} \right)^3 + \dots + \frac{1}{n+1} \left(\frac{J_1}{J_m} \right)^{n+1} \right] \\ \Rightarrow W &= \frac{E}{6} \left[(I_1 - 3) + \frac{1}{2J_m}(I_1 - 3)^2 + \frac{1}{3J_m^2}(I_1 - 3)^3 + \dots \right] \\ \Rightarrow W &= \sum_{i=1}^{\infty} C_i (I_1 - 3)^i \end{aligned} \quad (34)$$

Similarly, Arruda-Boyce model can be re-written in terms of general invariant based form as follows

$$W = \sum_{i=1}^{\infty} C_i (I_1 - 3^i). \tag{35}$$

Eqs. 4.34 and 4.35 can be used to predict large stretch deformations.

There are many hyperelastic material models available. Some of them are presented in this section, while others were discussed in the previous section. Models such as Van der Waal and Marlow models have not been presented here because they do not show good convergence for swelling elastomers. Next section gives the comparison of different hyperelastic material models against experimental results from uniaxial tensile tests.

4. Comparison of material models under tensile loading

As none of the available material models accurately represents swelling elastomers, modeling of these elastomers based on current models can yield only approximate results. Before this, no evaluation of material models for prediction of swelling elastomer behavior could be found in published literature. This study was therefore conducted to have a comparative assessment of current hyperelastic material models; how closely they predict the actual behavior under tension. Two water swelling elastomers are used for experimental and numerical investigation under tension (material-TA and material-TB). Tests are carried out in accordance with ASTM-D412 standard test method [53]. Tensile tests are also simulated, using the commercial finite element package ABAQUS [54]. Simulations are done using different hyperelastic material models available in the ABAQUS materials library. Material coefficients for each model are determined from experimental results using the curve fitting procedure of ABAQUS.

4.1 Experimental work

The main objective of the experimental work is to provide actual tensile test data to extract parameters for the material models, and then to compare predicted behavior from each model against the actual tensile behavior. A large number of samples of two different water-swelling elastomers were allowed to swell for 8 days in saline water of 40,000 ppm (4%) concentration at a temperature of 60°C (actual field conditions in a regional oil-well). Tensile tests were carried out on ring samples before and after swelling, reported values being average of readings from three samples. As expected, the material expands due to swelling. Dimensions of the ring samples before and after swelling are shown in **Figure 2**.

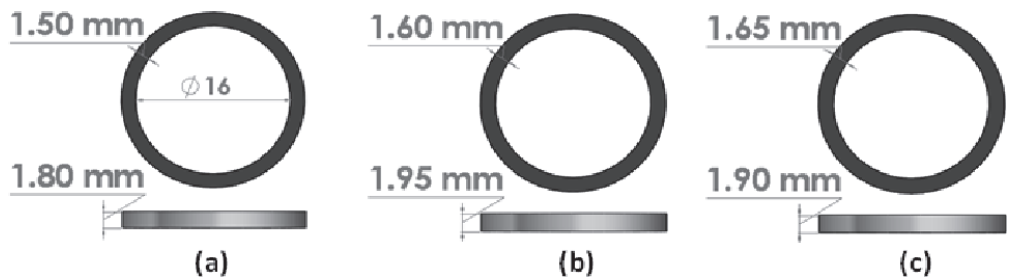


Figure 2.
Samples before and after swelling: (a) before swelling, (b) material TA after swelling, (c) material TB after swelling.

4.1.1 Sample preparation

Ring samples were cut in line with ASTM-D412, using a die-and-punch set; outside diameter (d_o) 19 mm, inside diameter (d_i) 16 mm, radial width (w) 1.5 mm, and thickness (t) 1.8 mm. Actual identification numbers of the two swelling-elastomer materials are not mentioned here due to reasons of confidentiality; they are simply referred to as material *TA* and material *TB*.

4.1.2 Test procedure

Width, thickness, and flattened length of all ring samples (before and after swelling) are recorded prior to conducting the tensile test, to be used later for stress and strain measurements. Specially fabricated (in-house) hook-type fixtures (in accordance with ASTM D412) are used to grip the ring samples. A small pre-tension is applied on each sample to get the flattened length as shown in **Figure 3**. A loading rate of 500 mm/min is used until the sample ruptures. Force-elongation and stress-strain readings are automatically recorded by the machine.

4.2 Numerical Modeling and simulation

Tensile tests are modeled and simulated using the commercial finite element package ABAQUS. Standard dumbbell shaped tensile specimen is used for simulation because of its symmetric nature, allowing modeling of only one-quarter of the sample; **Figure 4**. Load application is also simplified because of this sample geometry, yielding proper uni-axial tension. Swelling elastomer specimen is modeled as a hyperelastic body using 8-noded linear brick element with reduced integration (C3D8R). Deformed specimen is also shown in **Figure 4**. Minor inconsistencies between experimental and simulated results can be expected, as the sample geometries (ring-type and dumbbell-type) are different.

Four well-known material models (Ogden, Yeoh, Arruda-Boyce, and neo-Hookean) are selected from the pool of hyperelastic models available in ABAQUS. These are known to show convergence and good agreement with experimental data for elastomeric materials under tension. Coefficients for each model are extracted from the uniaxial tensile test data (experimental) using curve fitting techniques. Poisson's ratio for these elastomers has been taken as $\nu = 0.495$, while density values (from actual experiments) for un-swelled (US) and swelled (S) specimens of materials *TA* and *TB* are $\rho_{US-TA} = 1170 \text{ kg/m}^3$, $\rho_{US-TB} = 1187 \text{ kg/m}^3$, $\rho_{S-TA} = 1282 \text{ kg/m}^3$, and $\rho_{S-TB} = 1293 \text{ kg/m}^3$, respectively.



Figure 3.
Tensile test setup using elastomer ring samples; different stages of testing.

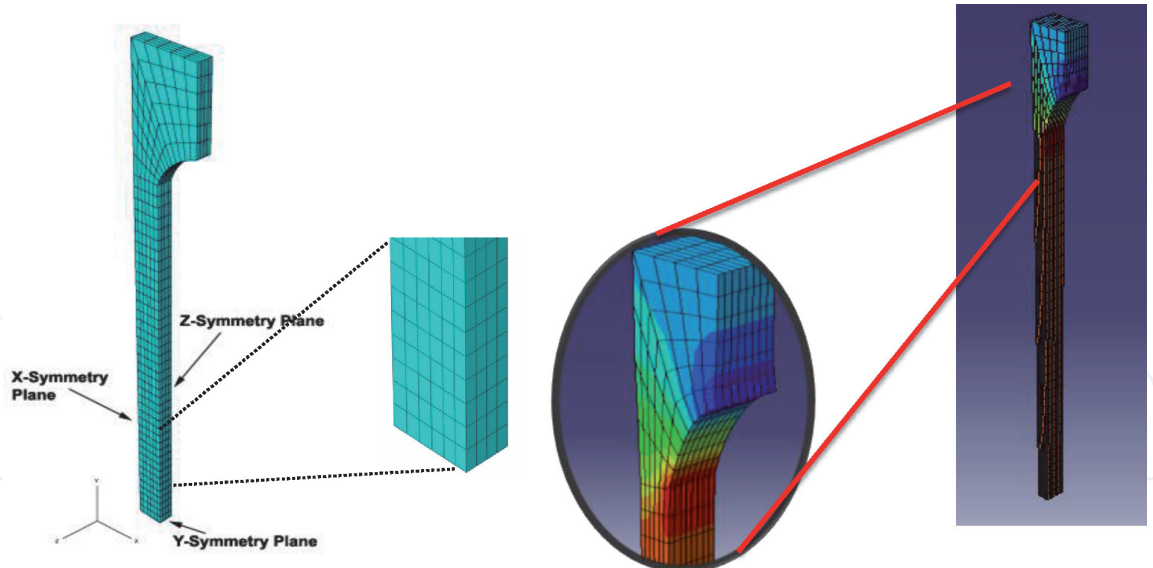


Figure 4.
Finite element model, and deformed shape, of dumbbell type test specimen.

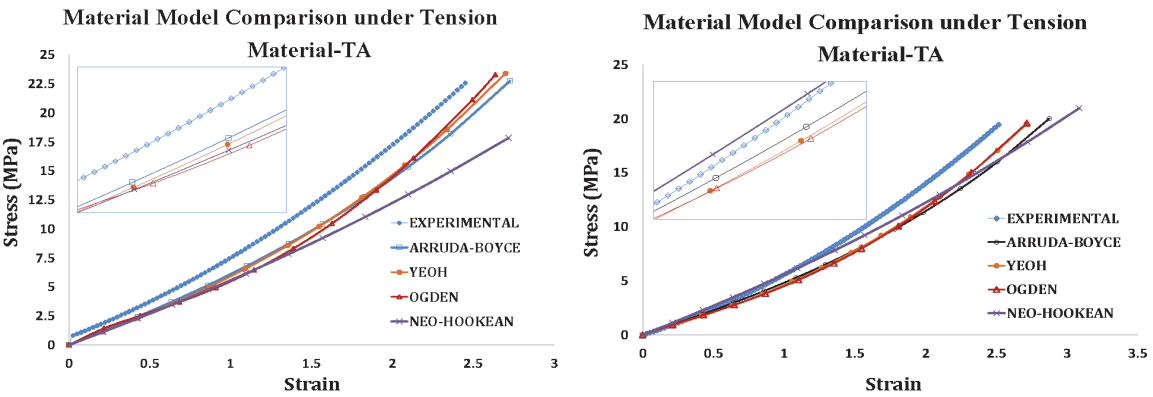


Figure 5.
Stress–strain curves for experimental and FE simulation results for material TA; before swelling (left); after 8 days of swelling (right).

4.3 Results and discussion

For both materials, finite element simulation of uni-axial tensile test is done using the four most popular material models for the un-swelled and 8-day swelled conditions. Stress–strain curves from simulations, using the selected material models, are compared with experimental results. Results are plotted separately for materials *TA* and *TB*. During the tensile tests, elastomer *TB* exhibited more stiffness, fracturing at much lower strains than elastomer *TA*.

Figure 5 shows comparison of stress–strain curves for experimental and FE simulation data for un-swelled and swelled (8 days) conditions for material *TA*. In the unswelled condition, at small deformations, all models predict almost the same behavior, Ogden model giving minimum error. For small to medium deformation, Arruda-Boyce model gives minimum error. For large deformations, Ogden model gives minimum error. After 8 days of swelling, for small deformations, all the models again predict almost the same behavior, Arruda-Boyce and neo-Hookean models yielding minimum error. For small to medium deformations, Neo-Hookean model gives the closest results. For large deformations, Ogden model again yields minimum error, Neo-Hookean model giving much larger error.

For material *TB*, experimental and simulated stress–strain curves for un-swelled and 8-day-swelled samples are shown in **Figure 6**. Before swelling, and at small

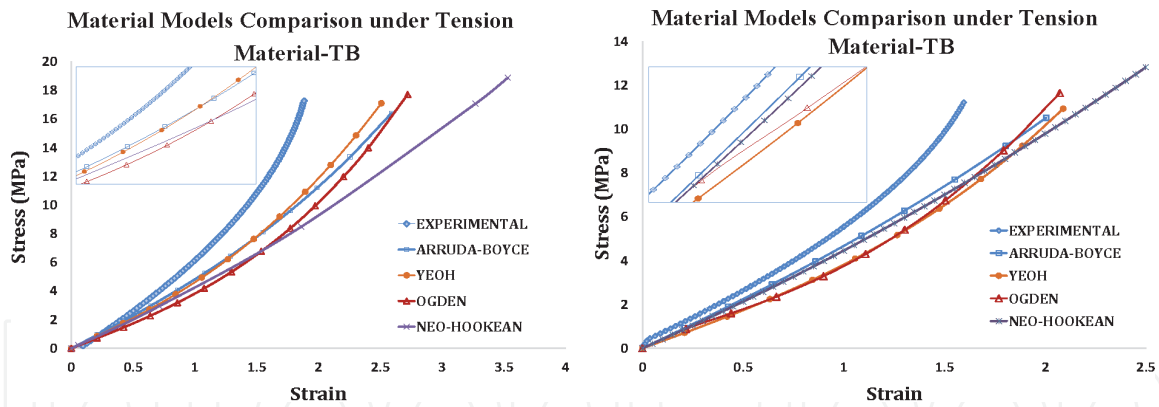


Figure 6. Stress–strain curves for experimental and FE simulation results for material TB; before swelling (left); after 8 days of swelling (right).

deformations, all models are very close to each other, Arruda-Boyce giving the best fit. The trend remains the same for small to medium deformations. For large deformations, Yeoh model gives the closest results. After swelling for 8 days, Arruda-Boyce model shows the closest fit to actual data for small deformations, the other models giving slightly higher error. The trend continues for small to medium deformations. For large deformations, Arruda-Boyce curve starts to diverge away from experimental results while Ogden and Yeoh models show converging tendency, Ogden model yielding the minimum error.

Based on results of the current study, the neo-Hookean model appears to be the best suited for both un-swelled and swelled (small to medium stretch) conditions under tensile loads, but it starts diverging away from experimental results for very large strains. For large strains (which is the case in real-world use of swelling elastomer seals), Ogden model is consistently better than the others. However, it can be seen that no material model predicts results close to the experimental values. The reason might be that energy and diffusion effects are not considered in these models.

5. Comparison of material models under compressive loading

Petroleum industry uses swelling elastomers in a variety of applications as discussed in detail in Chapter 2. Being primarily used as a sealing element, swelling elastomers generally experience compressive loads. Hence, investigation of such elastomers under compression is very important. A comparison of currently available hyperelastic material models is presented in this section against experimental results for two swelling elastomers (A and B) under compressive loading, before and after different stages of swelling. Just as for tensile loading, such an evaluation of material models for swelling elastomers under compression was not available in published literature before this study. Tests are carried out using disc samples in accordance with ASTM-D575 standard test method [55]. Compression tests are also simulated using the different material models available in the commercial finite element package ABAQUS [54]. Material coefficients for each model are determined from experimental stress–strain data using the curve fitting procedure of ABAQUS.

5.1 Experimental work

To replicate actual field conditions in many regional oil wells, Qamar et al. [56, 57] used samples of two types of water-swelling elastomers in various

petroleum development applications were subjected to swelling in saline water of 0.6% (6,000 ppm) and 12% (120,000 ppm) concentrations maintained at a temperature of 50°C. To investigate the effect of swelling, samples were taken out for mechanical testing after 1, 2, 4, 7, 10, 16, 23, and 30 days of swelling. The elastomers were of a fast-swelling type, so readings were initially taken after almost each day, and on a weekly basis later on.

5.1.1 Sample preparation

Disc samples were cut using a die-and-punch set, with some surface grinding needed for final trimming. As prescribed by ASTM-D575, disc dimensions for compression testing are 28.5 mm diameter and 12.5 mm thickness. Due to reasons of confidentiality, actual identification number of swelling-elastomer materials is not mentioned here.

5.1.2 Test procedure

Compression tests are performed on a Tinius Olsen universal testing machine in the compression mode, using a 50-kN load cell; **Figure 7**. Disc specimen is placed on a fixed bottom plate while the top plate applies a compressive load on the specimen. Elastomer sample is free to expand in the radial direction. Top surface of the disc moves downward with the compression load, while bottom surface is not allowed to move in the axial direction. Load is applied at a rate of 12 mm/min (ASTM-D575) until the specimen thickness is compressed to 10 mm. Force-deformation and stress-strain data are recorded. A small barreling effect can be observed in the compressed sample.

5.2 Numerical Modeling and simulation

Finite element analysis for predicting the deformation behavior of swelling elastomers under compression for both the materials in two salinities solutions are performed using commercial finite element analysis package ABAQUS [54]. Swelling elastomer specimen is modeled using 8-noded linear brick element with reduced integration (C3D8R). Stress-strain data obtained from experiments are used to extract coefficients that define the constitutive relation in finite element analysis. Material parameters such as Poisson's ratio and density at each condition with swelling for different days are also determined experimentally. ASTM standard disc



Figure 7.
Setup for compression testing, using disc samples.

geometry is modeled for simulation of compression tests. Compressive loads and boundary conditions are in line with experimental values. Simulations are conducted before swelling and after each swelling period for a total of one month period under both salinities. **Figure 8** shows the deformed and undeformed specimens.

5.3 Results and discussion

Finite element simulations of compression experiments are carried out for comparison of the five most suitable hyperelastic material models, including Ogden model with both first and second strain energy functions. Stress–strain curves obtained through simulations (for both the materials) are compared against experimental results after each swelling period.

Experimental and numerical stress–strain curves are compared in **Figure 9**, for material *A* in high salinity solution after 23 days of swelling. Apart from the five models shown in the figure, other material models failed to converge. For small deformations (10–15%), all models give quite good prediction. However, for medium to large deformations, none of the models is even remotely close to experimental results. Compared to the others, Yeoh and Ogden model with second strain energy function ($N = 2$) are relatively closer to the experimental curve, Ogden being the better one.

Experimental stress–strain curves for material *B* are compared with simulation results in **Figure 10** for low salinity solution after 30 days of swelling. Arruda-Boyce model failed to converge. Neo-Hookean and Ogden (with first strain energy potential) models are nowhere close to the experimental results. Yeoh and Ogden (strain energy potential of second degree) models give somewhat better results for small to moderate deformations. None of the models is good at large strains.

Experimental investigation of performance of swelling elastomer seals (such as sealing pressure at various stages of swelling) is highly difficult and very costly. Numerical simulations, if yielding reasonable predictions, can be a much better alternative. If we want to conduct numerical studies of elastomer seal performance, Ogden model with second-degree strain energy function will have to be used as it gives overall best results both under tensile and compressive loads. This best available current hyperelastic model (Ogden-2) has been later used to study the mechanical and structural behavior of swelling elastomers under compressive

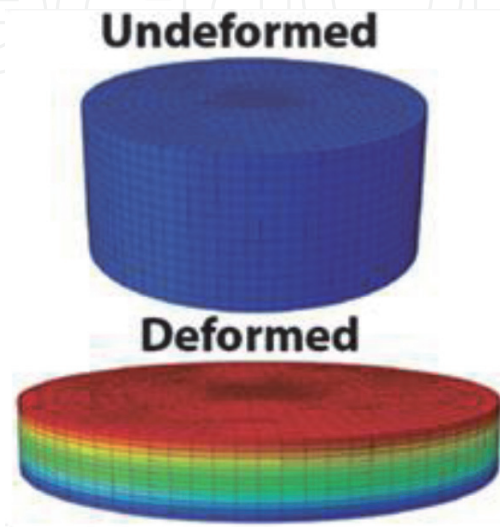


Figure 8.
Specimen (FE simulation) before and after deformation.

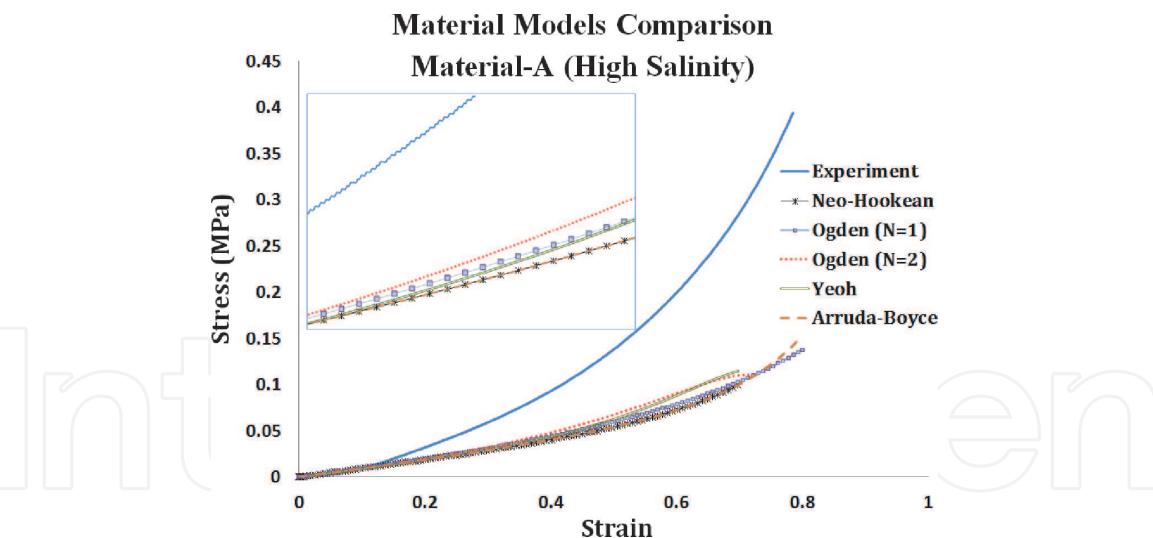


Figure 9.
Comparison of experimental and simulated (different hyperelastic material models) stress–strain behavior under compression for material A in high salinity after 23 days of swelling.

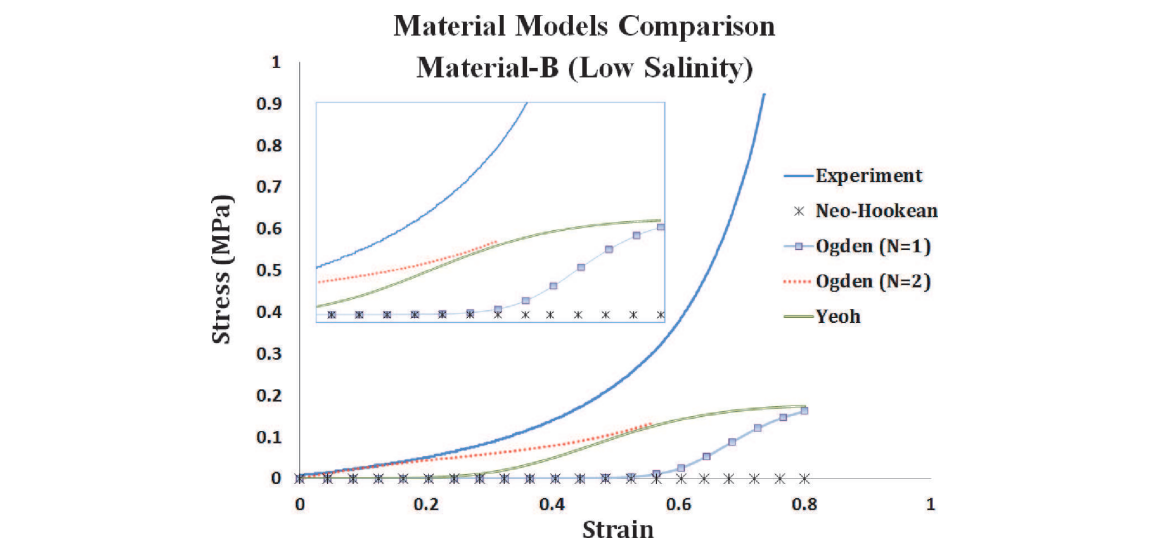


Figure 10.
Comparison of experimental and simulated (different hyperelastic material models) stress–strain behavior under compression for material B in low salinity after 30 days of swelling.

loading in Chapter 7, and to evaluate the performance of swelling elastomer seals in Chapter 8.

To more accurately predict the behavior of swelling elastomers, thermodynamics of mixing and the phenomenon of diffusion should also be considered. Starting with the Ogden model, this approach for mechanics of swelling is followed in Chapter-6 to develop a new material model for swelling elastomers.

6. Conclusions

Simulations have been carried out to compare different hyperelastic material models against experimental results for swelling elastomers subjected to tensile and compressive loading, including Arruda-Boyce, Ogden ($N = 1$), Ogden ($N = 2$), Yeoh, and neo-Hookean models. Following ASTM standards, experiments were conducted on ring samples (for tensile tests) and disc samples (for compression tests), before swelling, and after 8 days of swelling, using two swelling elastomer

materials. Simulations were performed using the FEA package ABAQUS. For tensile loads, most of the models give reasonable predictions for small deformations. For medium to large deformations, Ogden model with second strain energy function (Ogden-2) gives best results. For simulations under compression, many models do not give good predictions even for small loads. Ogden-2 again yields overall minimum error. Hyperelastic models can be used for FE analysis of swellables, giving reasonably acceptable approximations. However, a new material model is definitely needed to capture the material behavior of swelling elastomers more accurately.

Author details


Sayyad Zahid Qamar^{1*}, Maaz Akhtar² and Tasneem Pervez¹

1 Mechanical and Industrial Engineering Department, Sultan Qaboos University, Muscat, Oman

2 Mechanical Engineering Department, N.E.D. University of Engineering and Technology, Karachi, Pakistan

*Address all correspondence to: sayyad@squ.edu.om

IntechOpen

© 2021 The Author(s). Licensee IntechOpen. Distributed under the terms of the Creative Commons Attribution - NonCommercial 4.0 License (<https://creativecommons.org/licenses/by-nc/4.0/>), which permits use, distribution and reproduction for non-commercial purposes, provided the original is properly cited. 

References

- [1] Kuhn W, Grün F (1942) "Beziehungen Zwischen Elastischen Konstanten und Dehnungsdoppelbrechung Hochelastischer Stoffe," *Kolloid-Zeitschrift*, 101(3), 248-271.
- [2] Wall FT (1942) "Statistical Thermodynamics of Rubber," *Rubber chemistry and technology*, 15(3), 468-472.
- [3] Flory PJ, Rehner Jr J (1943) "Statistical Mechanics of Cross-Linked Polymer Networks: Rubberlike Elasticity," *Journal of Chemical Physics*, 11, 512-520.
- [4] Flory P, Rehner J (1943) "Statistical Mechanics of Cross-Linked Polymer Networks II. Swelling," *Journal of Chemical Physics*, 11, 521-526.
- [5] James H, Guth E (1943) "Theory of the Elastic Properties of Rubber," *Journal of Chemical Physics*, 11(10), 455-481.
- [6] Wang MC, Guth E (1952) "Statistical Theory of Networks of Non-Gaussian Flexible Chains," *Journal of Chemical Physics*, 20, 1144-1157.
- [7] Treloar L (1943) "The Elasticity of a Network of Long-Chain Molecules — II," *Transactions of the Faraday Society*, 39, 241-246.
- [8] Arruda EM, Boyce MC (1993) "A Three-Dimensional Constitutive Model for the Large Stretch Behavior of Rubber Elastic Materials," *Journal of the Mechanics and Physics of Solids*, 41(2), 389-412.
- [9] Wu P, Van der Giessen E (1992) "On Improved 3-D Non-Gaussian Network Models for Rubber Elasticity," *Mechanics Research Communications*, 19(5), 427-433.
- [10] Mooney M (1940) "A Theory of Large Elastic Deformation," *Journal of Applied Physics*, 11, 582-592.
- [11] Rivlin, R. (1948). Large elastic deformations of isotropic materials. Iv. Further developments of the general theory. *Philosophical Transactions of the Royal Society of London. Series A, Mathematical and Physical Sciences*, 241 (835), 379-397.
- [12] Treloar L (1944) "Stress-Strain Data for Vulcanised Rubber under Various Types of Deformation," *Transactions of the Faraday Society*, 40, 59-70.
- [13] Boyce MC, Arruda EM (2000) "Constitutive Models of Rubber Elasticity: A Review," *Rubber chemistry and technology*, 73(3), 504-523.
- [14] Kilian H-G (1980) "A Molecular Interpretation of the Parameters of the Van der Waals Equation of State for Real Networks," *Polymer Bulletin*, 3(3), 151-158.
- [15] Gent A (1996) "A New Constitutive Relation for Rubber," *Rubber Chemistry and Technology*, 69(1), 59-61.
- [16] Yeoh O, Fleming P (1997) "A New Attempt to Reconcile the Statistical and Phenomenological Theories of Rubber Elasticity," *Journal of Polymer Science-B Polymer Physics Edition*, 35(12), 1919-1932.
- [17] Marlow R (2003) "A General First-Invariant Hyperelastic Constitutive Model," *Constitutive Models for Rubber*, 157-160.
- [18] Ogden R (1972) "Large Deformation Isotropic Elasticity — On the Correlation of Theory and Experiment for Incompressible Rubberlike Solids," *Proceedings of the Royal Society of London. A.*

Mathematical and Physical Sciences, 326 (1567), 565-584.

[19] Twizell E, Ogden R (1983) "Non-Linear Optimization of the Material Constants in Ogden's Stress-Deformation Function for Incompressible Isotropic Elastic Materials," The Journal of the Australian Mathematical Society. Series B. Applied Mathematics, 24(04), 424-434.

[20] Ali A, Hosseini M, Sahari B (2010) "A Review of Constitutive Models for Rubber-like Materials," American Journal of Engineering and Applied Sciences, 3(1), 232.

[21] Hossain M, Steinmann P (2013) "More Hyperelastic Models for Rubber-Like Materials: Consistent Tangent Operators and Comparative Study," Journal of the Mechanical Behavior of Materials, 22(1-2), 27-50.

[22] Steinmann P, Hossain M, Possart G (2012) "Hyperelastic Models for Rubber-Like Materials: Consistent Tangent Operators and Suitability for Treloar's Data," Archive of Applied Mechanics, 82(9), 1183-1217.

[23] Treloar LRG (1975) The physics of Rubber Elasticity, Oxford University Press.

[24] Flory PJ, Erman B (1982) "Theory of Elasticity of Polymer Networks," Macromolecules, 15(3), 800-806.

[25] Boyce MC, Arruda EM (2001) "Swelling and Mechanical Stretching of Elastomeric Materials," Mathematics and Mechanics of Solids, 6(6), 641-659.

[26] Wagner M (1994) "The Origin of the C2 Term in Rubber Elasticity," Journal of Rheology (1978-present), 38 (3), 655-679.

[27] Han WH, Horka F, McKenna GB (1999) "Mechanical and Swelling Behaviors of Rubber: A Comparison of

Some Molecular Models with Experiment," Mathematics and Mechanics of Solids, 4(2), 139-167.

[28] Cai S, Suo Z (2012) "Equations of State for Ideal Elastomeric Gels," EPL (Europhysics Letters), 97(3), 34009.

[29] Chester SA, Anand L (2010) "A Coupled Theory of Fluid Permeation and Large Deformations for Elastomeric Materials," Journal of the Mechanics and Physics of Solids, 58(11), 1879-1906.

[30] Drozdov A, Christiansen J (2013) "Constitutive Equations in Finite Elasticity of Swollen Elastomers," International Journal of Solids and Structures, 50(9), 1494-1504.

[31] Hong W, Zhao X, Zhou J, Suo Z (2008) "A Theory Of Coupled Diffusion And Large Deformation In Polymeric Gels," Journal of the Mechanics and Physics of Solids, 56(5), 1779-1793.

[32] Lucantonio A, Nardinocchi P, Teresi L (2013) "Transient Analysis of Swelling-Induced Large Deformations in Polymer Gels," Journal of the Mechanics and Physics of Solids, 61(1), 205-218.

[33] Flory PJ (1942) "Thermodynamics of High Polymer Solutions," Journal of Chemical Physics, 10, 51-61.

[34] Huggins ML (1942) "Some Properties of Solutions of Long-Chain Compounds," The Journal of Physical Chemistry, 46(1), 151-158.

[35] Hong W, Liu Z, Suo Z (2009) "Inhomogeneous Swelling of a Gel in Equilibrium with a Solvent and Mechanical Load," International Journal of Solids and Structures, 46(17), 3282-3289.

[36] Kang MK, Huang R (2010) "A Variational Approach and Finite Element Implementation for Swelling of Polymeric Hydrogels under Geometric

Constraints,” *Journal of Applied Mechanics*, 77(6), 061004.

[37] Biot MA (1941) “General Theory of Three-Dimensional Consolidation,” *Journal of Applied Physics*, 12, 155-164.

[38] Cai S, Hu Y, Zhao X, Suo Z (2010) “Poroelectricity of a Covalently Crosslinked Alginate Hydrogel under Compression,” *Journal of Applied Physics*, 108(11), 113514.

[39] Lucantonio A, Nardinocchi P (2012) “Reduced Models of Swelling-Induced Bending of Gel Bars,” *International Journal of Solids and Structures*, 49(11), 1399-1405.

[40] Tomari T, Doi M (1994) “Swelling Dynamics of a Gel undergoing Volume Transition,” *Journal of the Physical Society of Japan*, 63(6), 2093-2101.

[41] Barrière B, Leibler L (2003) “Kinetics of Solvent Absorption and Permeation through a Highly Swellable Elastomeric Network,” *Journal of Polymer Science Part B: Polymer Physics*, 41(2), 166-182.

[42] Baek S, Pence T (2011) “Inhomogeneous Deformation of Elastomer Gels in Equilibrium under Saturated and Unsaturated Conditions,” *Journal of the Mechanics and Physics of Solids*, 59(3), 561-582.

[43] Bouklas N, Huang R (2012) “Swelling Kinetics of Polymer Gels: Comparison of Linear and Nonlinear Theories,” *Soft Matter*, 8(31), 8194-8203.

[44] Durning C, Morman Jr K (1993) “Nonlinear Swelling of Polymer Gels,” *The Journal of Chemical Physics*, 98(5), 4275-4293.

[45] Dolbow J, Fried E, Ji H (2004) “Chemically Induced Swelling of Hydrogels,” *Journal of the Mechanics and Physics of Solids*, 52(1), 51-84.

[46] Ji H, Mourad H, Fried E, Dolbow J (2006) “Kinetics of Thermally Induced Swelling of Hydrogels,” *International Journal of Solids and Structures*, 43(7), 1878-1907.

[47] Feynman R, Leighton R, Sands M (1963) *The Feynman Lectures on Physics*, Addison-Wesley

[48] Duda FP, Souza AC, Fried E (2010) “A Theory for Species Migration in a Finitely Strained Solid with Application to Polymer Network Swelling,” *Journal of the Mechanics and Physics of Solids*, 58(4), 515-529.

[49] Yan H, Jin B (2012) “Influence of Microstructural Parameters on Mechanical Behavior of Polymer Gels,” *International Journal of Solids and Structures*, 49(3), 436-444.

[50] Wu P, van der Giessen E (1995) “On Neck Propagation in Amorphous Glassy Polymers under Plane Strain Tension,” *International Journal of Plasticity*, 11(3), 211-235.

[51] Valanis K, Landel R (1967) “The Strain-Energy Function of a Hyperelastic Material in terms of the Extension Ratios,” *Journal of Applied Physics*, 38(7), 2997-3002.

[52] Boyce MC (1996) “Direct Comparison of the Gent and the Arruda-Boyce Constitutive Models of Rubber Elasticity,” *Rubber chemistry and technology*, 69(5), 781-785.

[53] ASTM-D412-98a (1998), *Standard Test Methods for Vulcanized Rubber and Thermoplastic Elastomers: Tension*, American Society for Testing and Materials.

[54] ABAQUS (2012), *Software version 6.11: Dassault Systems*.

[55] ASTM-D575-91 (2007), *Standard Test Methods for Rubber Properties in*

Compression, American Society for Testing and Materials.

[56] Qamar SZ, Hiddabi SA, Pervez T, Marketz F (2009) "Mechanical Testing and Characterization of a Swelling Elastomer," *Journal of Elastomers and Plastics*, 41 (5), September 2009, p 415-431

[57] Qamar SZ, Pervez T, Akhtar M, Al-Kharusi MSM (2012) "Design and Manufacture of Swell Packers: Influence of Material Behavior," *Materials and Manufacturing Processes*, 27 (7), 2012, p 727-732